

Does Dinitrogen Hydrogenation Follow Different Mechanisms for $[(\eta^5\text{-C}_5\text{Me}_4\text{H})_2\text{Zr}]_2(\mu_2,\eta^2,\eta^2\text{-N}_2)$ and $\{[\text{PhP}(\text{CH}_2\text{SiMe}_2\text{NSiMe}_2\text{CH}_2)\text{PPh}]\text{Zr}\}_2(\mu_2,\eta^2,\eta^2\text{-N}_2)$ Complexes? A Computational Study

Petia Bobadova-Parvanova, Qingfang Wang, David Quinonero-Santiago,[†]
Keiji Morokuma,* and Djamaladdin G. Musaev*

Contribution from the Cherry L. Emerson Center for Scientific Computation and Department of Chemistry, Emory University, Atlanta, Georgia 30322

Received November 22, 2005; E-mail: morokuma@emory.edu; dmusaev@emory.edu

Abstract: The mechanisms of dinitrogen hydrogenation by two different complexes— $[(\eta^5\text{-C}_5\text{Me}_4\text{H})_2\text{Zr}]_2(\mu_2,\eta^2,\eta^2\text{-N}_2)$, synthesized by Chirik and co-workers [*Nature* **2004**, 427, 527], and $\{[\text{P}_2\text{N}_2]\text{Zr}\}_2(\mu_2,\eta^2,\eta^2\text{-N}_2)$, where $\text{P}_2\text{N}_2 = \text{PhP}(\text{CH}_2\text{SiMe}_2\text{NSiMe}_2\text{CH}_2)_2\text{PPh}$, synthesized by Fryzuk and co-workers [*Science* **1997**, 275, 1445]—are compared with density functional theory calculations. The former complex is experimentally known to be capable of adding more than one H_2 molecule to the side-on coordinated N_2 molecule, while the latter does not add more than one H_2 . We have shown that the observed difference in the reactivity of these dizirconium complexes is caused by the fact that the former ligand environment is more rigid than the latter. As a result, the addition of the first H_2 molecule leads to two different products: a non-H-bridged intermediate for the Chirik-type complex and a H-bridged intermediate for the Fryzuk-type complex. The non-H-bridged intermediate requires a smaller energy barrier for the second H_2 addition than the H-bridged intermediate. We have also examined the effect of different numbers of methyl substituents in $[(\eta^5\text{-C}_5\text{Me}_n\text{H}_{5-n})_2\text{Zr}]_2(\mu_2,\eta^2,\eta^2\text{-N}_2)$ for $n = 0, 4$, and 5 ($n = 5$ is hypothetical) and $[(\eta^5\text{-C}_5\text{H}_2\text{-1,2,4-Me}_3)(\eta^5\text{-C}_5\text{Me}_5)_2\text{Zr}]_2(\mu_2,\eta^2,\eta^2\text{-N}_2)$ and have shown that all complexes of this type would follow a similar H_2 addition mechanism. We have also performed an extensive analysis on the factors (side-on coordination of N_2 to two Zr centers, availability of the frontier orbitals with appropriate symmetry, and inflexibility of the catalyst ligand environment) that are required for successful hydrogenation of the coordinated dinitrogen.

1. Introduction

The design and synthesis of a novel catalyst that is capable of hydrogenating molecular nitrogen under mild conditions is of great fundamental and industrial interest.¹ The strong and nonpolar $\text{N}\equiv\text{N}$ triple bond, as well as the large HOMO–LUMO energy gap of the N_2 molecule, makes dinitrogen utilization very difficult and forces scientists and engineers to use extreme conditions for production of ammonia. In fact, the almost-century-old Haber–Bosch process utilizing N_2 and H_2 molecules to produce ammonia requires high temperature (400–650 °C) and high pressure (200–400 atm)² but still remains the most economical industrial process for ammonia production. Extensive studies during the past several decades have not yet led to the discovery of an economically more effective nitrogen fixation process from N_2 and H_2 molecules.¹ However, new and promising reactions have been discovered.^{3–5} For instance,

Fryzuk and co-workers³ have demonstrated that the dinuclear Zr complex $\{[\text{P}_2\text{N}_2]\text{Zr}\}_2(\mu_2,\eta^2,\eta^2\text{-N}_2)$, **Fr_1** (Figure 1a), where $\text{P}_2\text{N}_2 = \text{PhP}(\text{CH}_2\text{SiMe}_2\text{NSiMe}_2\text{CH}_2)_2\text{PPh}$, reacts under room conditions with one H_2 molecule and forms $\{[\text{P}_2\text{N}_2]\text{Zr}\}_2(\mu_2,\eta^2,\eta^2\text{-NNH})(\mu\text{-H})$, **Fr_A7**, with bridging hydride and hydrazido units.³ Detailed computational studies of a small model of this compound (**s_Fr_1**, Figure 1b), where the $\text{PhP}(\text{CH}_2\text{SiMe}_2\text{NSiMe}_2\text{CH}_2)_2\text{PPh}$ ligand is modeled by $(\text{PH}_3)_2(\text{NH}_3)_2$,⁶ have revealed that the reaction of **s_Fr_1** (and **Fr_1**, respectively) with H_2 occurs via “metathesis” transition state involving Zr, N, and two H atoms. More importantly, these computational studies have shown that the dinuclear Zr complex can add even more (two and three) H_2 molecules under appropriate experimental conditions.⁶ This theoretical prediction, however, has not yet been tested experimentally for **Fr_1**. Instead, Chirik and co-workers⁴ have achieved addition of a second and third H_2 molecule to a different dinuclear Zr complex, $[(\eta^5\text{-C}_5\text{Me}_4\text{H})_2\text{Zr}]_2(\mu_2,\eta^2,\eta^2\text{-N}_2)$, **4_Ch_1**⁷ (Figure 1d).

[†] Present address: Department of Chemistry, Universitat de les Illes Balears, 07122 Palma de Mallorca, Spain.

(1) (a) Fryzuk, M. D.; Johnson, S. A. *Coord. Chem. Rev.* **2000**, 200–202, 379. (b) *Catalytic Ammonia Synthesis*; Jennings, J. R., Ed.; Plenum: New York, 1991. (c) Fryzuk, M. D. *Nature* **2004**, 427, 498. (d) Shaver, M. P.; Fryzuk, M. D. *Adv. Synth. Catal.* **2003**, 345, 1061. (e) Schlögl, R. *Angew. Chem., Int. Ed.* **2003**, 42, 2004. (f) Musaev, D. G. *J. Phys. Chem. B* **2004**, 108, 10012. (g) Mori, M. *J. Organomet. Chem.* **2004**, 689, 4210. (2) *Encyclopedia Britannica*; Encyclopedia Britannica Inc.: Chicago, 1997.

(3) Fryzuk, M. D.; Love, J. B.; Retting, S. J. *Science* **1997**, 275, 1445. (4) Pool, J. A.; Lobkovsky, E.; Chirik, P. J. *Nature* **2004**, 427, 527. (5) Bernskoetter, W. H.; Lobkovsky, E.; Chirik, P. J. *J. Am. Chem. Soc.* **2005**, 127, 14051. (6) (a) Basch, H.; Musaev, D. G.; Morokuma, K. *J. Am. Chem. Soc.* **1999**, 121, 5754. (b) Basch, H.; Musaev, D. G.; Morokuma, K. *Organometallics* **2000**, 19, 3393.

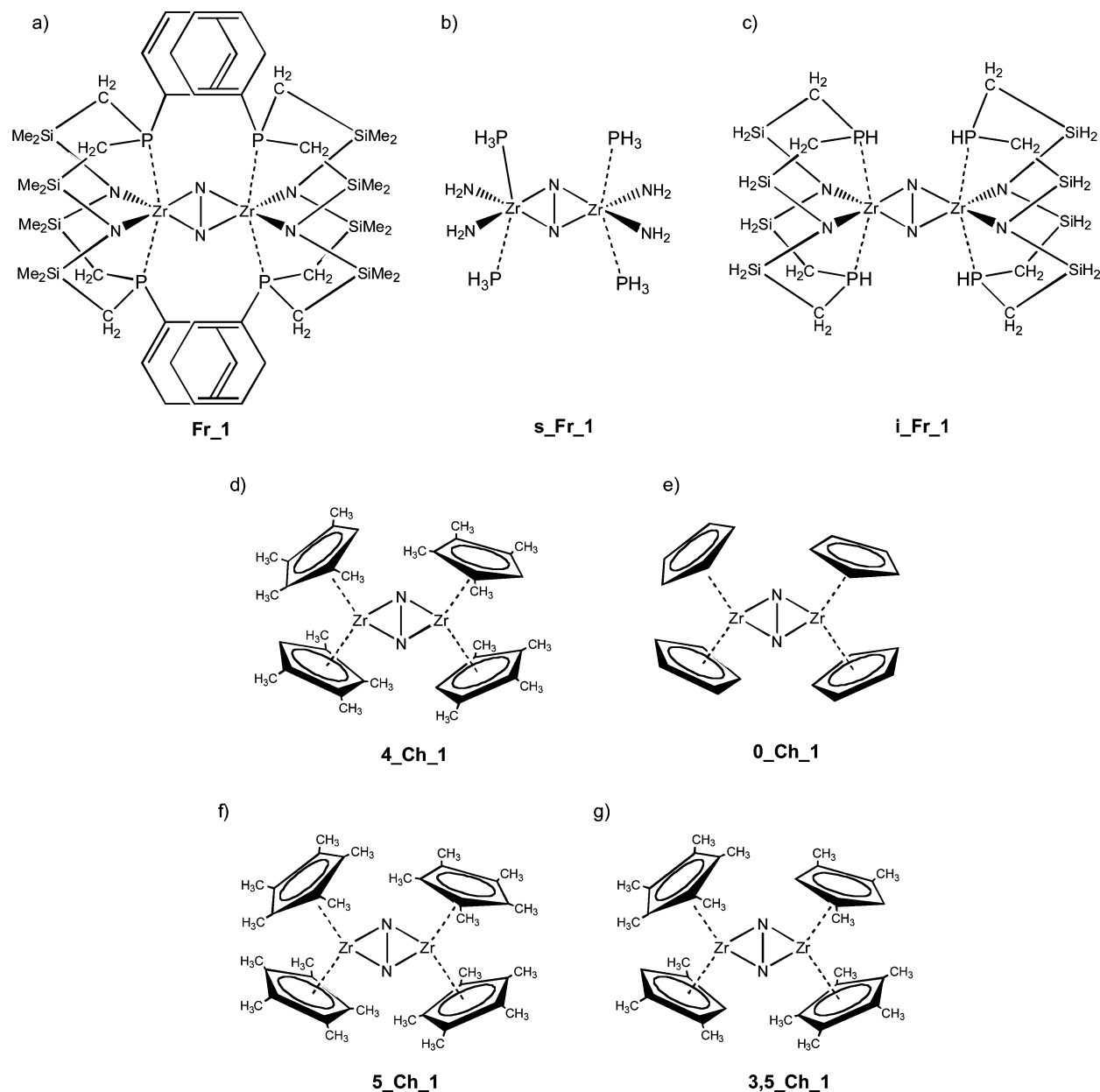


Figure 1. Schematic representation of (a) $\{[\text{P}(\text{H}(\text{C}_5\text{H}_4\text{SiMe}_2\text{NSiMe}_2\text{CH}_2)_2\text{PPh}]_2\text{Zr}\}_2(\mu_2, \eta^2, \eta^2\text{-N}_2)$ (**Fr_1**), (b) small model $\{[(\text{PH}_2)_2(\text{NH}_2)_2]\text{Zr}\}_2(\mu_2, \eta^2, \eta^2\text{-N}_2)$ (**s_Fr_1**), (c) intermediate model $\{[\text{HP}(\text{CH}_2\text{SiH}_2\text{NSiH}_2\text{CH}_2)_2\text{PH}]\text{Zr}\}_2(\mu_2, \eta^2, \eta^2\text{-N}_2)$ (**i_Fr_1**), (d) tetramethylated $[(\eta^5\text{-C}_5\text{Me}_4\text{H})_2\text{Zr}]_2(\mu_2, \eta^2, \eta^2\text{-N}_2)$ (**4_Ch_1**), (e) unmethylated $[(\eta^5\text{-C}_5\text{H}_5)_2\text{Zr}]_2(\mu_2, \eta^2, \eta^2\text{-N}_2)$ (**0_Ch_1**), (f) hypothetical side-on coordinated pentamethylated $[(\eta^5\text{-C}_5\text{Me}_5)_2\text{Zr}]_2(\mu_2, \eta^2, \eta^2\text{-N}_2)$ (**5_Ch_1**), and (g) mixed-ligand $[(\eta^5\text{-C}_5\text{H}_2\text{-1,2,4-Me}_3)(\eta^5\text{-C}_5\text{Me}_5)_2\text{Zr}]_2(\mu_2, \eta^2, \eta^2\text{-N}_2)$ (**3,5_Ch_1**).

This reaction has occurred at only 22 °C and 1 atm and has led to the formation of N–H bonds. Subsequent warming of the complex to 85 °C has even resulted in formation of a small amount of ammonia. Very recently, the same group reported a similar reactivity of the first and second H_2 additions to $[(\eta^5\text{-C}_5\text{H}_2\text{-1,2-Me}_3\text{-4-R})(\eta^5\text{-C}_5\text{Me}_5)_2\text{Zr}]_2(\mu_2, \eta^2, \eta^2\text{-N}_2)$ ($\text{R} = \text{Me, Ph}$) complexes.⁵

The reactions examined by Fryzuk and co-workers³ and Chirik and co-workers^{4,5} are still not catalytic, but their significance and practical importance are indisputable. These reactions have raised several very intriguing questions. Why, under room conditions, is **4_Ch_1** able to react with more than one H_2 molecule and even allows formation of a small amount

of ammonia, whereas **Fr_1** does not add more than one H_2 molecule? Does this mean that the two complexes follow different N_2 hydrogenation mechanisms? What causes this difference in their reactivity? To answer these questions, we need to understand the dinitrogen hydrogenation mechanism of **4_Ch_1** and how it compares with the dinitrogen hydrogenation mechanism of **Fr_1**.

The experiment of Chirik and co-workers⁴ itself raises a series of very interesting questions. Although the complex **4_Ch_1** (Figure 1d), with tetramethylated cyclopentadienyl ligands, $\text{C}_5\text{Me}_4\text{H}^-$, reacts with several H_2 molecules via the dinitrogen hydrogenation pathway, the pentamethylated complex, having C_5Me_5^- ligands, loses the N_2 unit when exposed to dihydrogen.⁸ In other words, replacing only one methyl group with hydrogen

(7) In this notation, the first number indicates the number of methyl substituents in each cyclopentadienyl ring of the ligand.

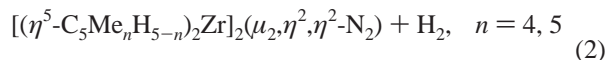
(8) Manriquez, J. M.; Bercaw, J. E. *J. Am. Chem. Soc.* **1974**, *96*, 6229.

in $C_5Me_5^-$ ligands completely alters the reactivity of the resulting complex. Recently, we demonstrated that the major reason behind this remarkable difference in the reactivity of these complexes is the different coordination mode of the bridging (supposedly hydrogenated) N_2 molecule.⁹ This result is consistent with an earlier prediction by Musaev that side-on coordination to transition metal centers is a necessary condition for N_2 hydrogenation.^{1f} Our detailed studies of side-on and end-on coordinated $[(C_5Me_nH_{5-n})_2Zr]_2(N_2)$ complexes for $n = 0-5$ demonstrated that, for $n \leq 4$, the side-on coordination of N_2 is energetically more favorable. The electronic effects caused by the methyl substitution would favor side-on coordination. When $n = 5$, however, the accumulated steric repulsion between the methyl groups makes the side-on coordination (suitable for N_2 hydrogenation) less stable than the end-on coordination (unsuitable for hydrogenation). We surmised that this is the reason why, experimentally, the pentamethylated complex ($n = 5$) cannot hydrogenate N_2 . In addition, since for all $[(C_5Me_nH_{5-n})_2Zr]_2(N_2)$ complexes with $n \leq 4$ the side-on coordination is energetically more favorable than the end-on coordination, we predicted that complexes with $n = 0-3$ will show reactivity similar to that of the experimentally reported tetramethylated complex $[(\eta^5-C_5Me_4H)_2Zr]_2(\mu_2,\eta^2,\eta^2-N_2)$, **4_Ch_1**.

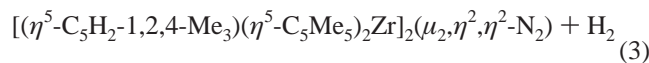
In the present paper, we further examine the role of methyl substitution for the dinitrogen hydrogenation mechanism. We study in detail the first, second, and third H_2 additions to the unmethylated complex $[(\eta^5-C_5H_5)_2Zr]_2(\mu_2,\eta^2,\eta^2-N_2)$, **0_Ch_1** (Figure 1e),



the first H_2 addition to the tetramethylated complex, **4_Ch_1** (Figure 1d), and the pentamethylated complex, **5_Ch_1** (Figure 1f),

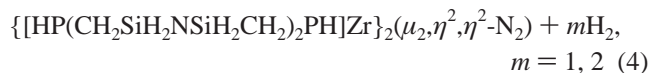


and the first H_2 addition to the recently synthesized complex $[(\eta^5-C_5H_2-1,2,4-Me_3)(\eta^5-C_5Me_5)_2Zr]_2(\mu_2,\eta^2,\eta^2-N_2)$, **3,5-Ch_1** (Figure 1g),



The most important goal of the present paper is to compare the mechanism of reactions 1-3 with the mechanism of H_2 addition to the complex **Fr_1**, synthesized by Fryzuk and co-workers. As mentioned above, the mechanism of dinitrogen hydrogenation at **Fr_1**, $\{[PhP(CH_2SiMe_2NSiMe_2CH_2)_2PPh]Zr\}_2(\mu_2,\eta^2,\eta^2-N_2)$ (Figure 1a), has been already modeled by **s_Fr_1** (Figure 1b), in which the $PhP(CH_2SiMe_2NSiMe_2CH_2)_2PPh$ ligands are replaced with $(PH_3)_2(NH_3)_2$.⁶ This model, however, is very small and requires some geometry constraints.⁶ Recently, Yates et al.¹⁰ performed a series of calculations using different levels of theory and a relatively large model of **Fr_1**. The authors showed that an intermediate model, **i_Fr_1** (Figure 1c), in which the $PhP(CH_2SiMe_2NSiMe_2CH_2)_2PPh$ ligand is replaced

by $HP(CH_2SiH_2NSiH_2CH_2)_2PH$, gives reasonable results. However, they did not investigate the full mechanism of the dinitrogen hydrogenation. For the purpose of the present paper, we study in detail the intermediates and transition states of the reaction of the H_2 addition to the intermediate model, **i_Fr_1**,



The present paper is organized as follows. In section 3.1 we examine in detail the first ($m = 1$), second ($m = 2$), and third ($m = 3$) H_2 additions to the unmethylated complex $[(\eta^5-C_5H_5)_2Zr]_2(\mu_2,\eta^2,\eta^2-N_2)$, **0_Ch_1** (reaction 1). In section 3.2 we study the mechanism of the first H_2 addition to the complexes $[(\eta^5-C_5Me_4H)_2Zr]_2(\mu_2,\eta^2,\eta^2-N_2)$, **4_Ch_1**, and $[(\eta^5-C_5Me_5)_2Zr]_2(\mu_2,\eta^2,\eta^2-N_2)$, **5_Ch_1** (reaction 2), and $[(\eta^5-C_5H_2-1,2,4-Me_3)(\eta^5-C_5Me_5)_2Zr]_2(\mu_2,\eta^2,\eta^2-N_2)$, **3,5_Ch_1** (reaction 3), and compare them with reaction 1. In section 3.3 we compare the mechanisms of reactions 1 and 4 and explain the reason for the different experimental reactivity of the complexes of Chirik and co-workers⁴ and Fryzuk and co-workers.³ At the end of the paper, in section 3.4, we discuss possible necessary conditions that would lead to successful dinitrogen hydrogenation.

2. Computational Procedure

All calculations were performed using the hybrid DFT B3LYP method¹¹ and the Stevens-Basch-Krauss (SBK)¹² relativistic effective core potentials (for Zr, C, N, Si, and P) and the standard CEP-31G basis sets for H, C, N, Si, P, and Zr atoms, with additional d-type polarization functions with exponent of 0.8 for all N atoms. Below we denote this approach as B3LYP/CEP-31G(d_N). This method allows straightforward comparison with previous computational studies of H_2 addition to dinuclear Zr complexes.⁶ The reliability of this approach has been tested in previous studies.⁶ The additional tests performed showed that the addition of polarization functions on all ligand atoms do not change significantly the relative energies of the examined potential energy surfaces. The reliability of the SBK¹² relativistic effective core potentials for C, N, Si, and P was tested by comparison of B3LYP/CEP-31G(d_N) performance with calculations using Stuttgart/Dresden (SDD)¹³ effective core potentials on Zr and the standard 6-31G(d) basis set on the remaining atoms (H, C, N, Si, P). The results show deviations of less than 1 kcal/mol in the relative energies of the investigated complexes (see Table 1S in the Supporting Information).

All structures were optimized without any symmetry constraints. The nature of all intermediates and transition states was confirmed performing normal-mode analysis and intrinsic reaction coordinate (IRC) calculations. To ensure effective comparison with previous calculations, below we discuss the energetics mainly without zero-point vibrational energy corrections (ZPC) and show values with ZPC in parentheses. All calculations were performed using the Gaussian 03 program package.¹⁴

(9) Bobadova-Parvanova, P.; Wang, Q.; Morokuma, K.; Musaev, D. G. *Angew. Chem., Int. Ed.* **2005**, *44*, 7101.
 (10) Yates, B. F.; Basch, H.; Musaev, D. G.; Morokuma, K. *J. Chem. Theory Comput.* **2006**, ASAP.

(11) (a) Becke, A. D. *Phys. Rev. A* **1988**, *38*, 3098. (b) Lee, C.; Yang, W.; Parr, R. G. *Phys. Rev. B* **1988**, *37*, 785. (c) Becke, A. D. *J. Chem. Phys.* **1993**, *98*, 5648.
 (12) (a) Stevens, W. J.; Basch, H.; Krauss, M. *J. Chem. Phys.* **1984**, *81*, 6026. (b) Stevens, W. J.; Krauss, M.; Basch, H.; Jasien, P. G. *Can. J. Chem.* **1992**, *70*, 612. (c) Cundari, T. R.; Stevens, W. J. *J. Chem. Phys.* **1993**, *98*, 5555.
 (13) (a) Fuentealba, P.; Preuss, H.; Stoll, H.; Szentpaly, L. V. *Chem. Phys. Lett.* **1989**, *89*, 418. (b) Wedig, U.; Dolg, M.; Stoll, H.; Preuss, H. In *Quantum Chemistry: The Challenge of Transition Metals and Coordination Chemistry*; Veillard, A., Ed.; Reidel: Dordrecht, 1986; p 79. (c) Leininger, T.; Nicklass, A.; Stoll, H.; Dolg, M.; Schwedtfeger, P. *J. Chem. Phys.* **1996**, *105*, 1052. (d) Cao, X. Y.; Dolg, M. *J. Mol. Struct. (THEOCHEM)* **2002**, *581*, 139.
 (14) Frisch, M. J.; et al. *Gaussian 03*, Revision C.02; Gaussian, Inc.: Wallingford, CT, 2004.

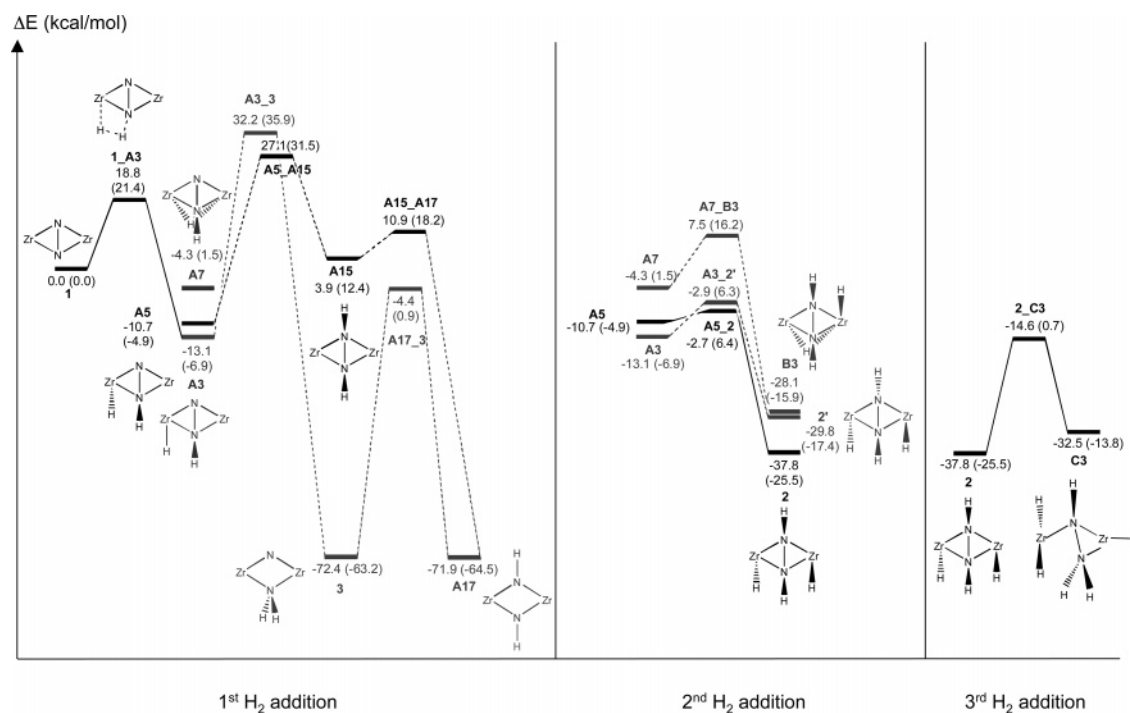


Figure 2. B3LYP/CEP-31G(dN) calculated potential energy profile without ZPC (in parentheses with ZPC) of the first, second, and third H₂ additions to [(η⁵-C₅H₅)₂Zr]₂(μ₂,η²,η²-N₂), **0_Ch_1**.

3. Results and Discussion

3.1. Mechanism of the First, Second, and Third H₂ Additions to Unmethylated [(η⁵-C₅H₅)₂Zr]₂(μ₂,η²,η²-N₂) Complex, **0_Ch_1.** The calculated potential energy surface (PES) profiles of reaction 1, the first, second, and third H₂ additions to [(η⁵-C₅H₅)₂Zr]₂(μ₂,η²,η²-N₂), **0_Ch_1**, are shown in Figure 2. The transition states and intermediates are named in accord with refs 6 and 10; the letters A, B, and C correspond to the first, second, and third H₂ addition, respectively. The name of each transition state indicates the two equilibrium states it connects. The most important equilibrium structures and transition states of reaction 1 and the values of the imaginary frequencies, as well as the energy barriers at the transition states, are presented in Figure 1S in the Supporting Information. Table 2S includes Cartesian coordinates of all calculated structures.

The addition of the first H₂ molecule to **0_Ch_1** results in formation of a diazenido complex, **0_Ch_A3**. This occurs via a “metathesis-like” transition state, **0_Ch_1_A3**, which includes breaking of one of the π(N–N) bonds and the H–H bond and formation of one Zr–H and one N–H bond. The formation of this transition state is in analogy with the mechanism determined by Basch et al.⁶ for the case of H₂ addition to **s_Fr_1**. The calculated barrier of the first H₂ addition to **0_Ch_1** is 18.8 kcal/mol. The reaction is exothermic by 13.1 kcal/mol. We distinguished three different isomers of the product. In **0_Ch_A3**, the two H atoms are located in syn position to each other. Its anti isomer, **0_Ch_A5**, where the H atoms point in opposite directions, is 2.4 kcal/mol higher in energy than **0_Ch_A3**. Another isomer is **0_Ch_A7**, where the H atom is in a bridging position between the two Zr centers. **0_Ch_A7** is 8.8 kcal/mol higher in energy than the nonbridging **0_Ch_A3**. Our calculations show that the barriers separating these three isomers, **0_Ch_A3**, **0_Ch_A5**, and **0_Ch_A7**, are very small. Scanning the PES showed that the migration of H from the syn position

in **0_Ch_A3** to the anti position in **0_Ch_A5** requires a barrier of only 2.5 kcal/mol. It could be expected that H-migration from the anti position in **0_Ch_A5** to the bridging position in **0_Ch_A7** would have a similar barrier. Transformation from **0_Ch_A5** to **0_Ch_A7** requires also twisting of the zirconocene edges from 51.0° to 3.4°, respectively. According to our previous study,⁹ such twisting needs only 0.06 kcal/mol. It could be concluded that the overall barrier for anti to bridging H-migration would be around 6.6 kcal/mol.

The thermodynamically more favorable product is neither of the diazenido isomers but the complexes **0_Ch_3**, with N and NH₂ bridging ligands, and **0_Ch_A17**, with two bridging NH ligands (Figure 2). However, these thermodynamically more favorable products are unlikely to be formed at the experimentally reported conditions (1 atm and 22 °C) because of the large energy barriers required for their formation: 45.3 kcal/mol at the **0_Ch_A3_3** transition state and 37.8 kcal/mol at the **0_Ch_A5_A15** transition state.

Instead, the reaction follows different paths. The products of the first H₂ addition reaction, complexes **0_Ch_A3**, **0_Ch_A5**, and **0_Ch_A7**, could react with a second H₂ molecule via “metathesis-like” transition states, **0_Ch_A3_2'**, **0_Ch_A5_2**, and **0_Ch_A7_B3**. These three transition states would lead to the formation of three different isomers, **0_Ch_2**, **0_Ch_2'**, and **0_Ch_B3**, respectively, having different mutual positions of the H atoms.¹⁵ The structures are shown schematically in Figure 2. Among them, structure **0_Ch_2** has the lowest energy (37.8 kcal/mol exothermic with respect to the initial reactants). This is in excellent agreement with the experiment, which confirms the formation of complex **0_Ch_2**.⁴

Analysis of these isomers indicates that the energetically most stable isomer, **0_Ch_2**, could be formed either directly from

(15) We are aware of the existence of additional isomers of **0_Ch_2**, which are not expected to contribute significantly to the hydrogenation of the coordinated N₂ molecule and are, therefore, not reported here.

the reaction of **0_Ch_A5** with a H₂ molecule (a second H₂ overall) or by isomerization of **0_Ch_2'**, the direct product of the reaction of **0_Ch_A3** with a H₂ molecule (again, a second H₂ overall). Since the **0_Ch_A3** to **0_Ch_A5** isomerization (barrier of 2.5 kcal/mol) is an easier process than the **0_Ch_2'** to **0_Ch_2** isomerization (barrier of around 14 kcal/mol¹⁶), the pre-reaction complex for the second H₂ addition is expected to be the isomer **0_Ch_A5**. Thus, our calculations show that the second H₂ addition occurs with a barrier of only 8.0 kcal/mol, which is less than half the first H₂ addition barrier (18.8 kcal/mol). The second H₂ addition is also more exothermic than the first one (27.1 vs 13.1 kcal/mol, respectively).

While preparing the current manuscript, we became aware of a very recent theoretical study by Miyachi et al.,¹⁶ where the authors used B3LYP/LanL2DZ calculations to investigate the first, second, and third H₂ additions to the complex **0_Ch_1**, as a model of the experimental **4_Ch_1** complex. The results for the first H₂ addition are in very good agreement with those from our study (barrier of 20.4 vs 18.8 kcal/mol). However, the second H₂ addition follows a different path. According to Miyachi et al., the isomer **0_Ch_A3** adds a second H₂ and produces the intermediate **0_Ch_2'**, with a barrier of 10.9 kcal/mol. **0_Ch_2'** is then transformed to the experimentally reported complex **0_Ch_2**. However, the **0_Ch_2'** → **0_Ch_2** isomerization requires a 13.8 kcal/mol barrier, which is slightly larger than that for the path proposed in the present study. Indeed, the pathway **0_Ch_A3** → **0_Ch_A5** → **0_Ch_2**, which we propose, requires only 2.5 kcal/mol for the first step (**0_Ch_A3** → **0_Ch_A5** isomerization) and 8.0 kcal/mol for the second step (**0_Ch_A5** + H₂ → **0_Ch_2**) (see Figure 2).

From **0_Ch_2**, the reaction may proceed via many pathways, leading to various products. However, we expect that the most feasible pathway should be an addition of the next (third) H₂ molecule. Here we study only the addition of a H₂ molecule (third overall) to the energetically most stable isomer **0_Ch_2**, which proceeds via a 23.2 kcal/mol energy barrier at the transition state **0_Ch_2_C3** and leads to the **0_Ch_C3** product. The reaction is endothermic by 5.3 kcal/mol. The product **0_Ch_C3** corresponds to structure C6 in ref 6.

3.2. Mechanism of the First H₂ Addition to Dinuclear Zirconocene Complexes with Different Numbers of Methyl Substituents. As discussed above, the tetramethylated and pentamethylated complexes show quite different reactivity.^{4,8} The tetramethylated complex leads to formation of N–H bonds, whereas the pentamethylated complex loses the N₂ molecule upon hydrogenation. Our recent paper⁹ showed that the reason for this difference lies in the side-on coordination (suitable for hydrogenation) of the tetramethylated complex and the end-on coordination (not suitable for hydrogenation) of the pentamethylated complex. The energetically less favorable side-on pentamethylated complex (**5_Ch_1**, Figure 1f) has the coordination that is suitable for hydrogenation. It could be expected that **5_Ch_1** would hydrogenate dinitrogen. Below we check this hypothesis. The N–H bond formation takes place at the first H₂ addition to complexes **4_Ch_1** (Figure 1d) and **5_Ch_1** (Figure 1f). Therefore, we investigate in detail only the first H₂ addition to the respective complex. In addition, we examine the first H₂ addition to another dinuclear zirconocene complex, **3,5_Ch_1** (Figure 1g), which was synthesized very recently.⁵

Experiment indicates that this complex shows reactivity similar to that of **4_Ch_1**. Below we check whether our calculations will confirm this finding.

Tetramethylated Dizirconium Complex, [(η⁵-C₅Me₄H)₂Zr]₂(μ₂,η²,η²-N₂), **4_Ch_1.** Recently, we discussed in detail the structure of the tetramethylated dinuclear [(η⁵-C₅Me₄H)₂Zr]₂(μ₂,η²,η²-N₂) complex, **4_Ch_1**.¹⁷ We analyzed different possible orientations of the four C₅HMe₄[−] ligands and demonstrated that, in agreement with experiment, the lowest energy structure of **4_Ch_1** is that in which the H substituents of the cyclopentadienyl ligands are oriented in opposite directions (see Figure 3, where the positions of the H atoms are indicated with arrows). The calculated and the experimentally reported geometric parameters (given in parentheses) are in very good agreement.

The addition of the first H₂ molecule to **4_Ch_1** proceeds with the formation of a transition state, **4_Ch_1_A3**, which, as could be expected, is similar to its unmethylated analogue, **0_Ch_1_A3** (Figure 3), and includes formation of one Zr–H bond and one N–H bond and breaking of one π bond of N₂ and the H–H bond of H₂. One should note that the symmetry of **4_Ch_1_A3** is lower than that of the reactant **4_Ch_1**. Therefore, we could expect multiple isomers of **4_Ch_1_A3**. Even if we account only for structures with the two H substituents pointing in opposite directions, there are still four distinguishable isomers of **4_Ch_1_A3**, connecting one and the same structure of **4_Ch_1** with the four different isomers of the product **4_Ch_A3**. These transition states could be viewed also as the H₂ molecule approaching the Zr₂N₂ core from its four different sides.

We examined all four isomers of **4_Ch_A3** and found that, in principle, the mechanism of the reaction remains unchanged and is not significantly influenced by the mutual orientation of the C₅HMe₄[−] ligands. As can be seen from Table 1, the barriers associated with these four different transition states vary within less than 2 kcal/mol, between 17.9 and 19.6 kcal/mol, or between 19.6 and 21.2 kcal/mol if we correct for the zero-point energy. More importantly, all calculated barriers for the reaction of tetramethylated complex **4_Ch_1** with H₂ are very similar to that for the reaction of **0_Ch_1** (18.8 kcal/mol). Thus, it seems that the existence of four methyl substituents in the cyclopentadienyl rings does not significantly influence the structure and energetics of the transition state of the first H₂ addition reaction.

As mentioned above, the four different **4_Ch_1_A3** transition states connect four different isomers of the product **4_Ch_A3**, which are energetically close to each other. As can be seen from Table 1, the exothermicity of the reaction **4_Ch_1** + H₂ → **4_Ch_A3** (11.5–17.6 kcal/mol) is comparable with that of **0_Ch_1** + H₂ (13.1 kcal/mol). Accounting for zero-point energy reduces the energetic differences between the four isomers to less than 3.5 kcal/mol.

Our calculations show that the potential energy profiles of the first H₂ addition to the unmethylated complex **0_Ch_1** and the tetramethylated complex **4_Ch_1** are very similar. In other words, the unmethylated complex **0_Ch_1** would react with a H₂ molecule in a manner similar to that of the experimentally studied tetramethylated complex **4_Ch_1**. Given the similarity between the reactions of the first H₂ with the unmethylated and

(16) Miyachi, H.; Shigeta, Y.; Hirao, K. *J. Phys. Chem. A* **2005**, *109*, 8800.

(17) Bobadova-Parvanova, P.; Quinero-Santiago, D.; Morokuma, K.; Musaeov, D. G. *J. Chem. Theory Comput.* **2006**, *2*, 336.

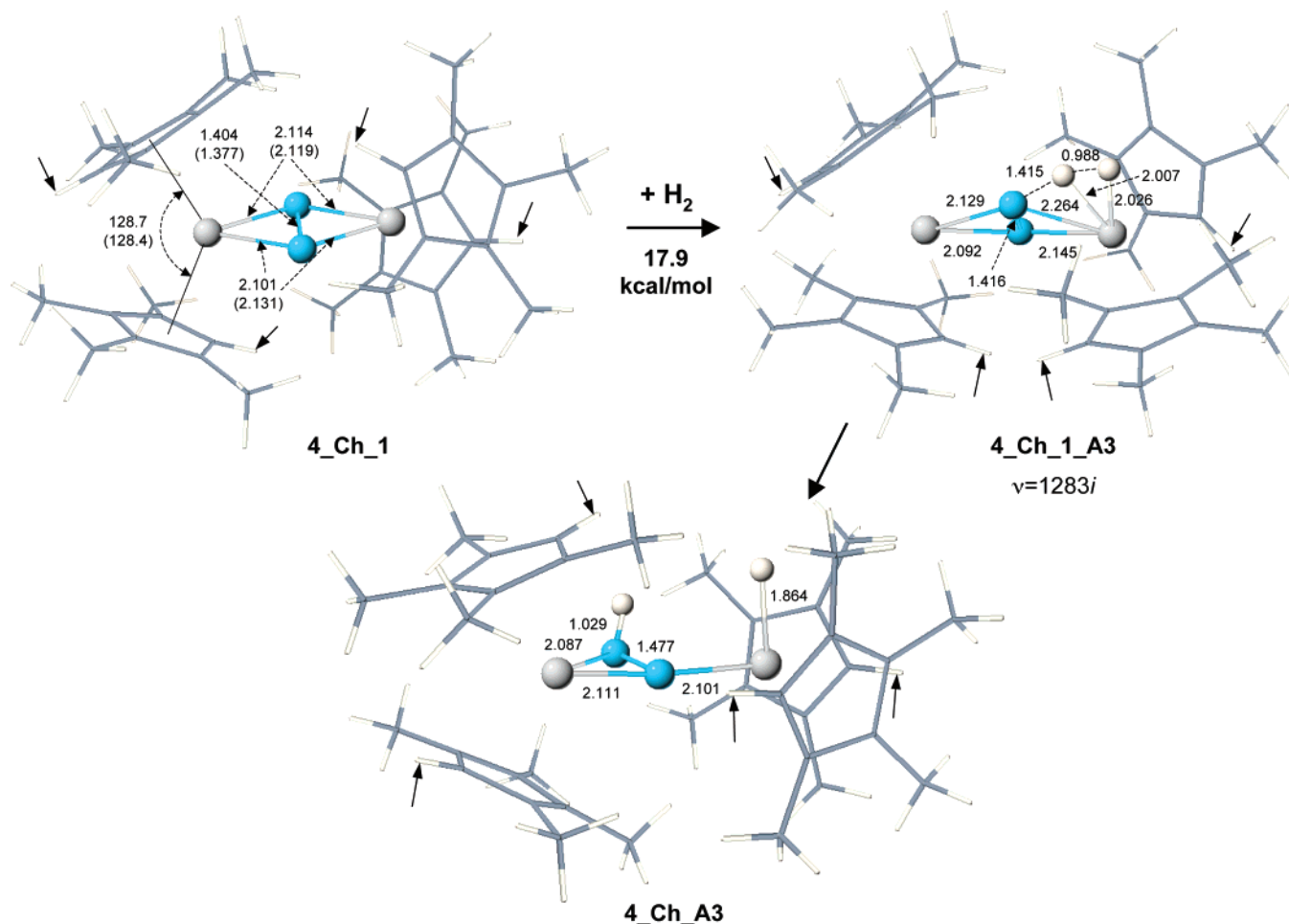


Figure 3. Tetramethylated $[(\eta^5\text{-C}_5\text{Me}_4\text{H})_2\text{Zr}]_2(\mu_2,\eta^2,\eta^2\text{-N}_2)$ complex. Optimized structures of (a) the lowest-energy isomer of reactant **4_Ch_1**, (b) the lowest-barrier transition state, **4_Ch_1_A3**, and (c) the product of the first H_2 addition, **4_Ch_A3**. Bond lengths are given in angstroms, angles in degrees. Experimental values are given in parentheses. The positions of the H atoms are indicated with arrows.

Table 1. B3LYP/CEP-31G(d_N) Calculated Relative Energies of Different Isomers of the Transition State **4_Ch_1_A3** and the Product **4_Ch_A3** of the First H_2 Addition to the Tetramethylated **4_Ch_1** Complex^a

| isomer | transition state 4_Ch_1_A3 | product 4_Ch_A3 |
|--------|--------------------------------------|---------------------------|
| 1 | 19.6 (21.2) | -17.1 (-5.4) |
| 2 | 18.7 (20.9) | -14.4 (-2.9) |
| 3 | 18.9 (20.3) | -17.6 (-6.3) |
| 4 | 17.9 (19.6) | -11.5 (-6.2) |

^a The energies are calculated with respect to the reactants and are given in kilocalories per mole. Zero-point corrected energies are given in parentheses.

tetramethylated complexes, we believe that the second and third H_2 additions would follow similar mechanisms.

Hypothetical Side-On Coordinated Pentamethylated Dzirconium Complex, $[(\eta^5\text{-C}_5\text{Me}_5)_2\text{Zr}]_2(\mu_2,\eta^2,\eta^2\text{-N}_2)$, **5_Ch_1.** Similar to the reactions of unmethylated and tetramethylated complexes, the reaction of a hypothetical side-on coordinated pentamethylated complex, **5_Ch_1**, with H_2 occurs via a “metathesis-like” transition state, **5_Ch_1_A3**, and leads to a N_2 hydrogenated product, **5_Ch_A3** (Figure 4). The calculated energy barrier for the pentamethylated complex **5_Ch_1** is 19.6 kcal/mol, which is only less than 2 kcal/mol higher than those of the unmethylated and tetramethylated complexes **0_Ch_1** and **4_Ch_1**. Therefore, the hypothetical side-on coordinated penta-

methylated complex would react with H_2 via the same mechanism as the unmethylated and tetramethylated complexes. This is additional evidence that the reason for the observed difference in the reactivity of the tetra- and pentamethylated dinuclear Zr complexes with H_2 is in the coordination mode of the N_2 molecule.

Since the side-on coordinated complexes **0_Ch_1**, **4_Ch_1**, and the hypothetical **5_Ch_1** follow one and the same mechanism of the first H_2 addition, it could be predicted that all side-on coordinated complexes $[(\eta^5\text{-C}_5\text{Me}_n\text{H}_{5-n})_2\text{Zr}]_2(\mu_2,\eta^2,\eta^2\text{-N}_2)$, for $n = 0-5$, would react similarly with H_2 . Whether experimentally a complex from this series is going to hydrogenate N_2 depends on the relative stability of the side-on and end-on coordinated complex for a given n . We showed previously⁹ that, for $n = 5$, the increased steric repulsion of the methyl substituents in the cyclopentadienyl ligands prevents the formation of the side-on coordinated complex, and the end-on complex is formed instead. Therefore, experimentally, the pentamethylated complex cannot hydrogenate dinitrogen. However, the side-on coordination of all complexes having $n \leq 4$ is more favorable than the end-on mode.⁹ Consequently, all $[(\eta^5\text{-C}_5\text{Me}_n\text{H}_{5-n})_2\text{Zr}]_2(\mu_2,\eta^2,\eta^2\text{-N}_2)$ complexes having $n \leq 4$ could activate the N_2 molecule for hydrogenation. We encourage experimentalists to check this theoretical prediction.

Mixed-Ligand Dzirconium Complex, $[(\eta^5\text{-C}_5\text{H}_2\text{-1,2,4-Me}_3)(\eta^5\text{-C}_5\text{Me}_5)_2\text{Zr}]_2(\mu_2,\eta^2,\eta^2\text{-N}_2)$, **3,5_Ch_1.** Figure 5 pre-

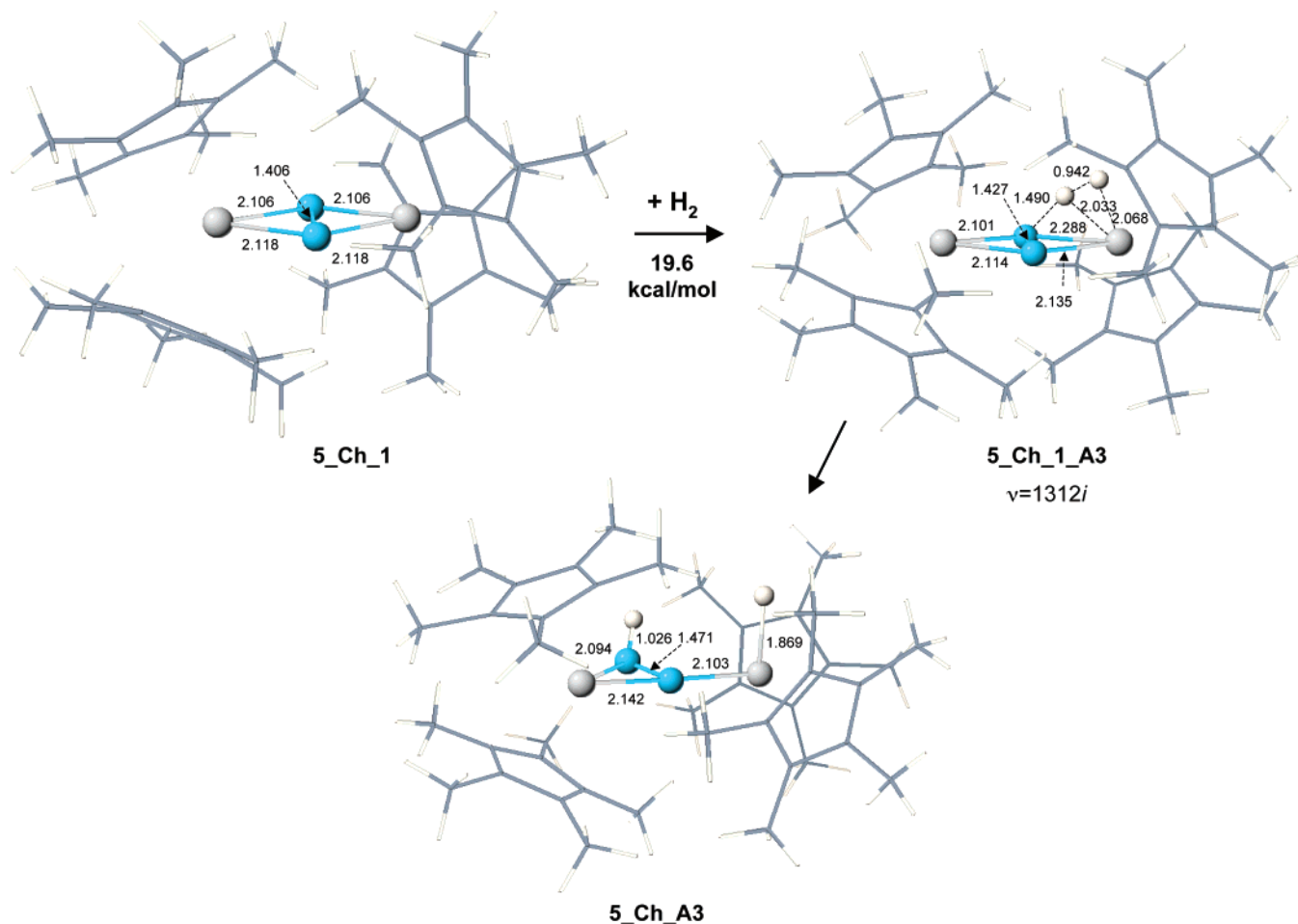


Figure 4. Hypothetical side-on coordinated pentamethylated $[(\eta^5\text{-C}_5\text{Me}_5)_2\text{Zr}]_2(\mu_2, \eta^2, \eta^2\text{-N}_2)$ complex. Optimized structures of (a) reactant **5_Ch_1**, (b) transition state **5_Ch_1_A3**, and (c) the product of the first H₂ addition, **5_Ch_A3**. Bond lengths are given in angstroms, angles in degrees.

sents the optimized structures of the reactant, transition state, and product of the first H₂ addition to the mixed-ligand dizirconium complex $[(\eta^5\text{-C}_5\text{H}_2\text{-1,2,4-Me}_3)(\eta^5\text{-C}_5\text{Me}_5)_2\text{Zr}]_2(\mu_2, \eta^2, \eta^2\text{-N}_2)$, **3,5_Ch_1**. This complex was synthesized very recently by Bernskoetter et al.⁵ It has three methyl substituents on two of its cyclopentadienyl rings and five methyl substituents on the other two. The authors reported that **3,5_Ch_1** shows reactivity similar to that of **4_Ch_1** for the addition of the first H₂ molecule, with **3,5_Ch_1** having a little lower reaction rate than **4_Ch_1** (1.2×10^{-3} vs 3.9×10^{-3} s⁻¹ at 0.647 atm of H₂ and 22 °C). Our study shows that the reaction of **3,5_Ch_1** with H₂ follows a mechanism similar to that of **4_Ch_1** (see Figure 3); a “metathesis-like” transition state is formed, which leads to the formation of a similar diazenido complex, **3,5_Ch_A3**. The calculated energy barrier is 19.8 kcal/mol, which is only 1.9 kcal/mol higher than that of the other experimentally studied complex, **4_Ch_1**. Although the energy difference is very small, our studies confirm the trend that **3,5_Ch_1** has a little lower reactivity toward H₂ addition than **4_Ch_1**.

3.3. Comparison of the Mechanisms of Dinitrogen Hydrogenation by Chirik-Type $[(\eta^5\text{-C}_5\text{H}_5)_2\text{Zr}]_2(\mu_2, \eta^2, \eta^2\text{-N}_2)$ and Fryzuk-Type $\{[\text{HP}(\text{CH}_2\text{SiH}_2\text{NSiH}_2\text{CH}_2)_2\text{PH}]\text{Zr}\}_2(\mu_2, \eta^2, \eta^2\text{-N}_2)$ Complexes. In the previous sections we have examined the hydrogenation of the coordinated N₂ by Chirik-type complexes $[(\eta^5\text{-C}_5\text{Me}_n\text{H}_{5-n})_2\text{Zr}]_2(\mu_2, \eta^2, \eta^2\text{-N}_2)$ for $n = 0$ and 4 (**0_Ch_1**, **4_Ch_1**), the hypothetical side-on coordinated pen-

tamethylated complex $[(\eta^5\text{-C}_5\text{Me}_5)_2\text{Zr}]_2(\mu_2, \eta^2, \eta^2\text{-N}_2)$ (**5_Ch_1**), and the mixed-ligand complex $[(\eta^5\text{-C}_5\text{H}_2\text{-1,2,4-Me}_3)(\eta^5\text{-C}_5\text{Me}_5)_2\text{Zr}]_2(\mu_2, \eta^2, \eta^2\text{-N}_2)$ (**3,5_Ch_1**). We have shown that, in principle, all complexes of this type follow similar reaction mechanisms. Now we will compare this mechanism with the H₂ addition to the Fryzuk type of complex, $\{[\text{PhP}(\text{CH}_2\text{SiMe}_2\text{NSiMe}_2\text{CH}_2)_2\text{PPh}]\text{Zr}\}_2(\mu_2, \eta^2, \eta^2\text{-N}_2)$ (**Fr_1**).

The experiments have revealed that **Fr_1** and **4_Ch_1** show different reactivities toward dinitrogen hydrogenation. Interestingly, **4_Ch_1** and **Fr_1** react similarly with the first H₂ molecule; both reactions lead to the formation of a N–H bond. However, the two complexes react differently upon consequent H₂ additions. **4_Ch_1** adds the second H₂ molecule and even produces a small amount of ammonia under subsequent gentle warming.⁴ On the other hand, although their feasibility under appropriate conditions has been predicted theoretically,⁶ the second and third H₂ additions to **Fr_1** have never been observed experimentally.³

The previous theoretical studies on **Fr_1**, $\{[\text{PhP}(\text{CH}_2\text{SiMe}_2\text{NSiMe}_2\text{CH}_2)_2\text{PPh}]\text{Zr}\}_2(\mu_2, \eta^2, \eta^2\text{-N}_2)$, were performed using a small model, **s_Fr_1**, in which the $\text{PhP}(\text{CH}_2\text{SiMe}_2\text{NSiMe}_2\text{CH}_2)_2\text{PPh}$ ligands were substituted by $(\text{PH}_3)_2(\text{NH}_3)_2$ (Figure 1b). To check the conclusions of these small model studies, in the present paper we re-investigate the first and second H₂ additions to an intermediate model of **Fr_1**, **i_Fr_1**, in which the $\text{PhP}(\text{CH}_2\text{SiMe}_2\text{NSiMe}_2\text{CH}_2)_2\text{PPh}$ ligands are substituted by $\text{HP}(\text{CH}_2\text{SiH}_2\text{NSiH}_2\text{CH}_2)_2\text{PH}$ (Figure 1c). According to recent results

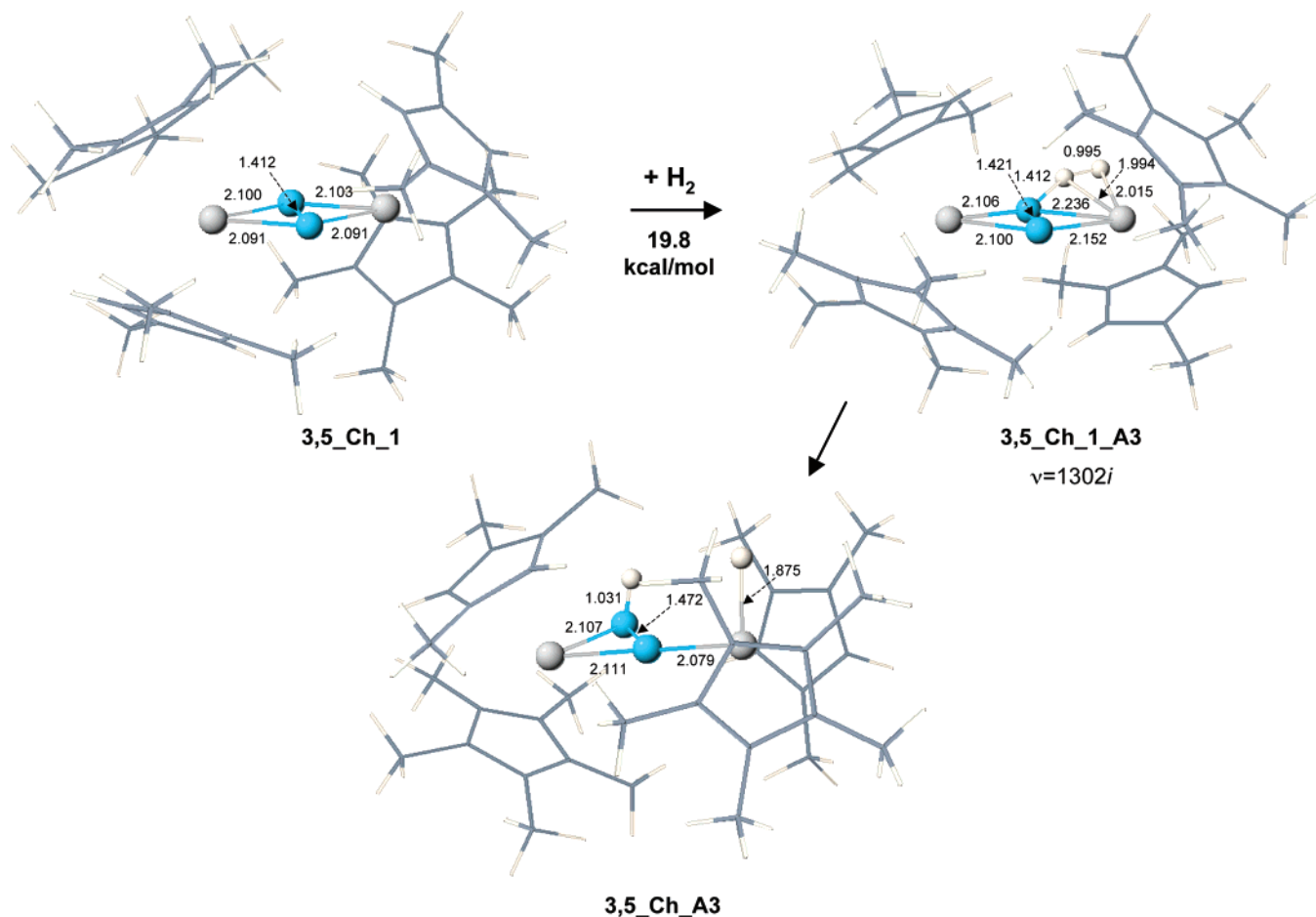


Figure 5. Mixed-ligand $[(\eta^5\text{-C}_5\text{H}_2\text{-1,2,4-Me}_3)(\eta^5\text{-C}_5\text{Me}_5)_2\text{Zr}]_2(\mu_2, \eta^2, \eta^2\text{-N}_2)$ complex. Optimized structures of (a) reactant **3,5_Ch_1**, (b) transition state **3,5_Ch_1_A3**, and (c) the product of the first H_2 addition, **3,5_Ch_A3**. Bond lengths are given in angstroms, angles in degrees.

reported by Yates et al.,¹⁰ this approximation provides a reasonable estimation of the PES of the complex. The previously performed calculations using the geometrically constrained small model (**s_Fr_1**) show a similar qualitative picture but differ from the presently used model (**i_Fr_1**) quantitatively. The small model also predicts that structure **A7** is more stable than **A3**, but the energy difference is only 8.0 kcal/mol. The intermediate model increases this difference to 16.5 kcal/mol. The barrier for the H_2 addition to **A7** is 29.9 kcal/mol for the intermediate model and 19.5 kcal/mol for the constrained small model. Overall, the conclusions of previous small model calculations are qualitatively acceptable, although the absolute values of energetics have to be modified.

Figure 6 compares the calculated potential energy profiles of the first and second H_2 additions to **i_Fr_1** and **0_Ch_1**. The most important equilibrium structures and transition states of the first and second H_2 additions to **i_Fr_1**, as well as the energy barriers at the transition states and the values of the imaginary frequencies, are presented in Figure 2S in the Supporting Information. Table 4S in the Supporting Information includes Cartesian coordinates of all structures. As can be seen from Figure 6, there are no substantial differences between **i_Fr_1** and **0_Ch_1** with respect to the first H_2 addition; both complexes lead to the formation of N–H bonds via “metathesis-like” transition states with barriers of 18.8 and 24.6 kcal/mol for **0_Ch_1** and **i_Fr_1**, respectively. This is in accord with the available experiments.^{3,4} The major difference in the

reactivity of **0_Ch_1** and **i_Fr_1** occurs *after* the first H_2 addition. The products of the reaction have three isomers with different mutual positions of the H atoms—a syn (**A3**), an anti (**A5**), and a μ -H (**A7**) isomer where one of the hydrogen atoms is located in a bridging position between the two Zr centers. The striking difference between the **0_Ch** and **i_Fr** series is the fact that the rearrangement **A3** \rightarrow **A5** \rightarrow **A7** is energetically favorable for the complex studied by Fryzuk and co-workers but is energetically unfavorable for the complex studied by Chirik and co-workers (Figure 6). The calculations show that the barriers separating these three isomers are very small. As already discussed in section 3.1, in the case of the **0_Ch** series, the H atom migrates from the syn position in **A3** to the anti position in **A5**. **A5** either adds a second H_2 molecule or rearranges to isomer **A7**. The rearrangement to **A7** requires around 6.6 kcal/mol. Due to the higher barrier (11.8 kcal/mol) for the second H_2 addition to **A7**, however, this reaction pathway, requiring a total of $6.6 + 11.8 = 18.4$ kcal/mol, will be realized with a smaller probability. Instead, the most probable pathway would be the second H_2 addition to **A5**. This process requires only 8.0 kcal/mol and leads to the formation of a very stable complex, **0_Ch_2** (relative energy of 27.1 kcal/mol with respect to the reactants **A5** + H_2). The stability of **0_Ch_2** provides a driving force for this reaction and is one of the reasons for the low barrier.

In the case of the **i_Fr** series, the H atom migrates from the syn position in **A3** to the anti position in **A5**, with a barrier of

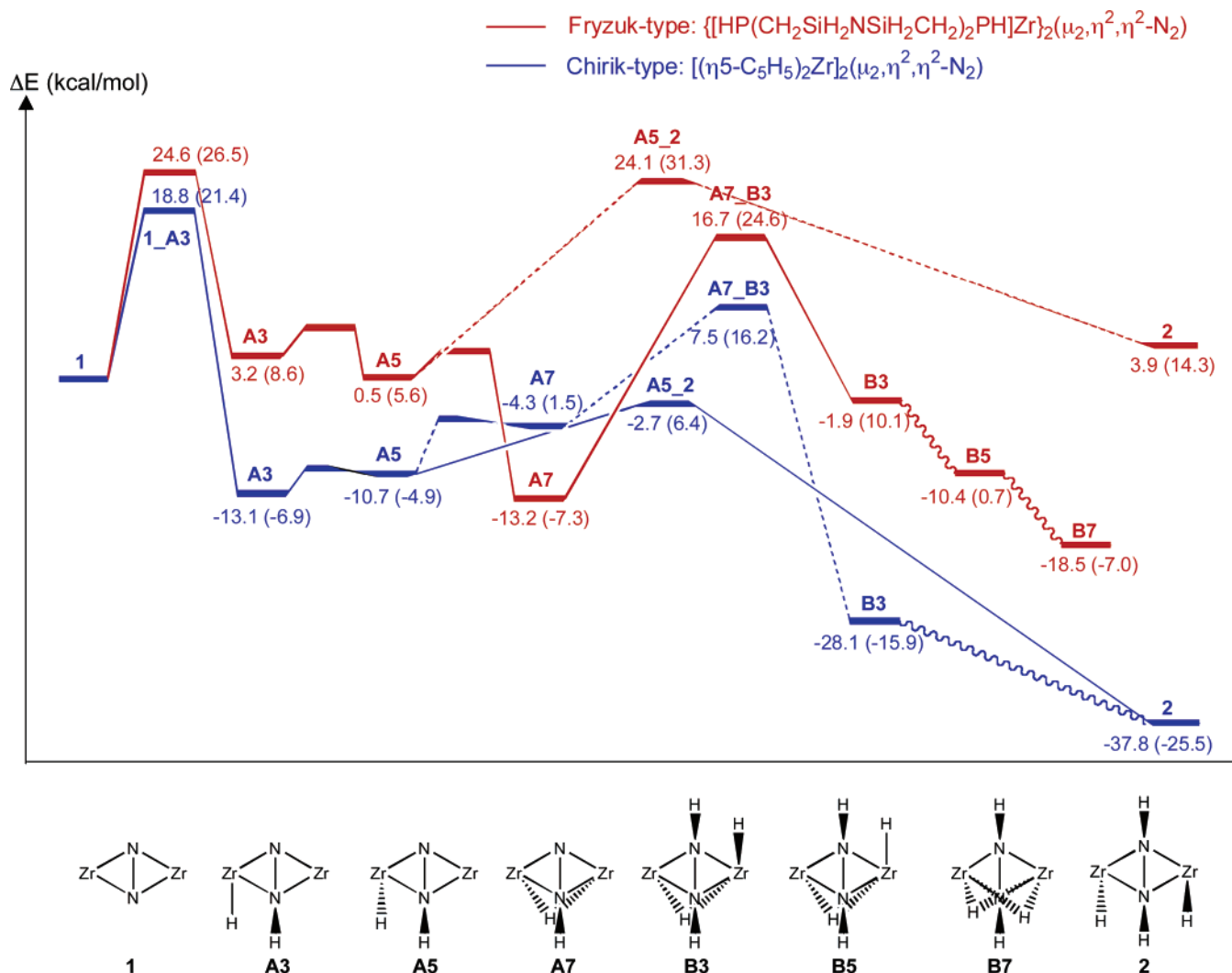


Figure 6. Comparison of the B3LYP/CEP-31G(d_K) potential energy profiles without ZPC (in parentheses with ZPC) for the first and the second H₂ additions to the Chirik-type complex, [(η⁵-C₅H₅)₂Zr](μ₂,η²,η²-N₂) (**0_Ch_1**), and the Fryzuk-type complex, {[HP(CH₂SiH₂NSiH₂CH₂)₂PH]Zr}₂(μ₂,η²,η²-N₂) (**i_Fr_1**).

4.1 kcal/mol. The barrier of H₂ addition to **A5** is high, 23.6 kcal/mol (Figure 6). Instead, **A5** transforms into the most stable H-bridged isomer **i_Fr_A7** with a barrier of only 3.3 kcal/mol. Isomer **i_Fr_A7** is 13.7 kcal/mol more stable than **i_Fr_A5** and 16.4 kcal/mol more stable than **i_Fr_A3**. Thus, in the case of Fryzuk-type complexes, the pre-reaction compound for the second H₂ addition is the most stable H-bridged isomer **i_Fr_A7**, rather than the non-H-bridged structures **A3** or/and **A5**, as in the case of **0_Ch_1**. The addition of a H₂ molecule to the H-bridged complex **i_Fr_A7** requires a significant (29.9 kcal/mol) barrier. The existence of such a large barrier explains why, under room conditions, the second H₂ addition to **Fr_1** has not been observed experimentally.

The above-reported difference in the products of H₂ addition to complexes **i_Fr_1** and **0_Ch_1** is consistent with the reported X-ray structures of possible intermediate species. Chirik and co-workers⁴ reported the formation of a non-H-bridged structure, **4_Ch_2** (tetramethylated analogue of **0_Ch_2**), whereas Fryzuk and co-workers reported the H-bridged **A7** type of intermediate.¹⁸

Our detailed theoretical calculations show that dinitrogen hydrogenation follows different mechanisms for the complexes studied by Fryzuk and co-workers³ and Chirik and co-workers.⁴ Indeed, addition of the first H₂ molecule to **i_Fr_1** results in the formation of a *very stable H-bridged intermediate A7*, which requires a *large energy barrier* for addition of the next H₂ molecule. In contrast, addition of the first H₂ to the **0_Ch_1** complex leads to the formation of *less stable non-H-bridged A3 or A5 complexes*, which react with the next H₂ molecule with a *much smaller energy barrier*. There are two important questions associated with these findings. First, why is the energetically most stable product of the reaction **i_Fr_1** + H₂ the H-bridged complex, while in the case of the **0_Ch** series the H-bridged structure is the less stable one? And second, why is the Fryzuk-type transition state of the second H₂ addition (**i_Fr_A7_B3**) much higher in energy than the respective Chirik-type transition state of the second H₂ addition (**0_Ch_A5_2**)?

To answer the first question we compared **i_Fr_A3** and **i_Fr_A7** with their analogues **0_Ch_A3** and **0_Ch_A7**. The optimized structures of these complexes are given in Figure 7. We decomposed the binding energy ΔE for addition of the H₂ molecule to **i_Fr_1** or **0_Ch_1**, respectively, into two components: deformation energy, *DEF*, representing the destabilization

(18) Basch, H.; Musaev, D. G.; Morokuma, K.; Fryzuk, M. D.; Love, J. B.; Seidel, W. W.; Albinati, A.; Koetzle, F.; Klooster, W. T.; Mason, S. A.; Eckert, J. *J. Am. Chem. Soc.* **1999**, *121*, 523.

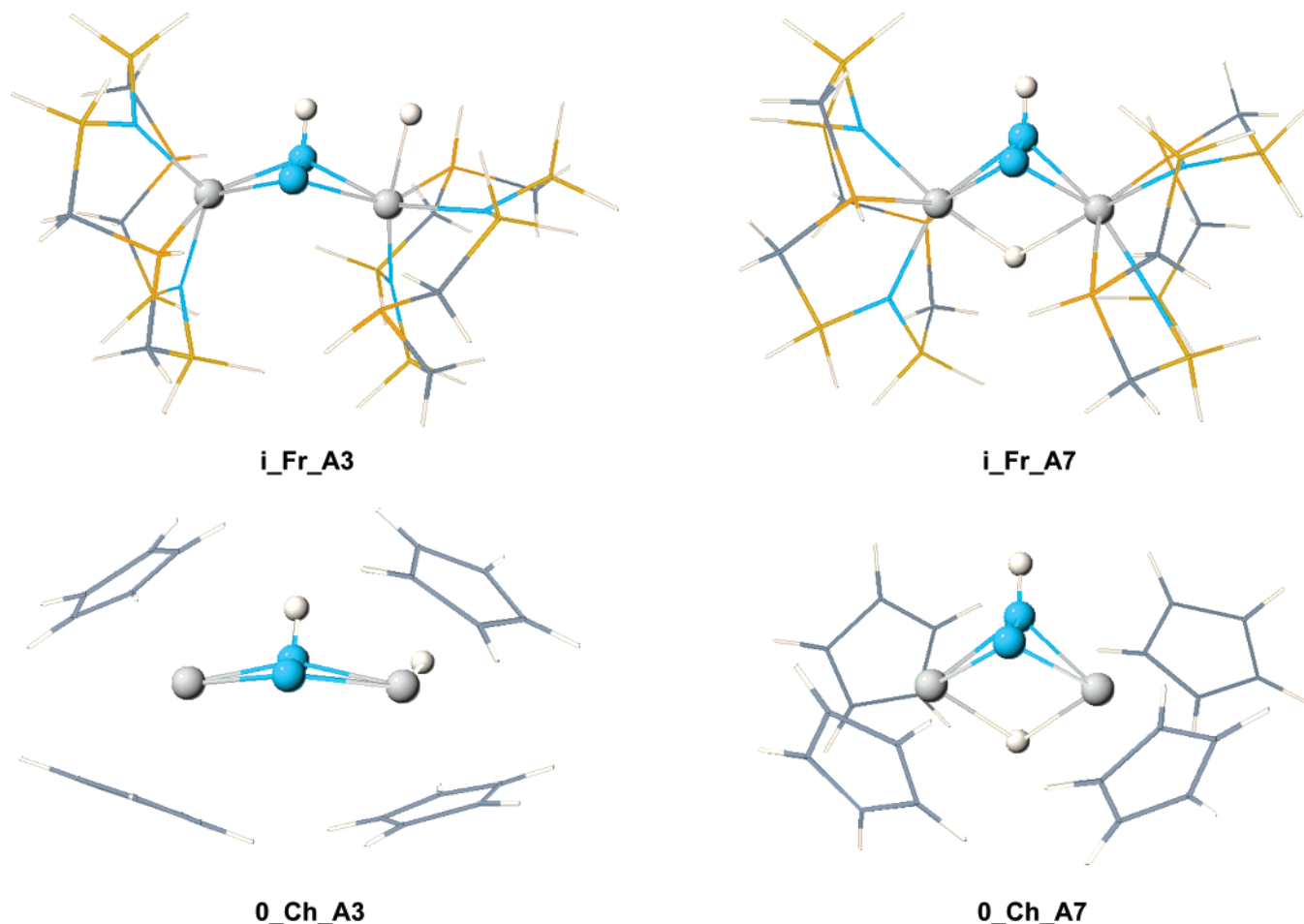


Figure 7. B3LYP/CEP-31G(d_N) optimized structures of the non-H-bridged complexes, **i_Fr_A3** and **0_Ch_A3**, and the H-bridged complexes, **i_Fr_A7** and **0_Ch_A7**, of the Fryzuk-type and Chirik-type compounds, respectively.

Table 2. Decomposition of the Stabilization Energy into Deformation and Interaction Energy, $\Delta E = DEF + INT$, for H-Bridged (**A7**) and Non-H-Bridged (**A3**) Complexes of the **I_Fr** and **0_Ch** Series^a

| | i_Fr series | | | 0_Ch series | | |
|-----------|-------------|------|-------|-------------|------|-------|
| | ΔE | DEF | INT | ΔE | DEF | INT |
| A3 | +3.2 | 23.9 | -20.7 | -13.1 | 19.6 | -32.7 |
| A7 | -13.2 | 33.2 | -46.4 | -4.3 | 62.3 | -66.6 |

^a The energies are calculated with respect to the reactants, **i_Fr_1** and **0_Ch_1**, respectively, and are given in kilocalories per mole.

energy due to the geometrical deformation of the two interacting fragments upon complexation, and pure interaction energy between the deformed fragments, *INT*. This is a simplified version of the Morokuma–Kitaura analysis.²² The results are shown in Table 2. As can be seen, in both cases the pure interaction energy, *INT*, is approximately twice as high (in absolute value) for the H-bridged **A7** complexes as for the non-H-bridged **A3** complexes: -46.4 vs -20.7 kcal/mol for the **i_Fr** series, and -66.6 vs -32.7 kcal/mol for the **0_Ch** series. This result is expected because of the existence of two Zr–H

interactions in the **A7**-type structures. Thus, interaction energy favors the bridging **A7** type of isomers for both **i_Fr** and **0_Ch**. However, the deformation energy changes the picture. Indeed, there is no significant difference in the deformation energy, *DEF*, required for formation of the non-H-bridged structures **i_Fr_A3** and **0_Ch_A3** for the two series of complexes; in both cases, *DEF* has approximately equal values, 23.9 vs 19.6 kcal/mol. However, the deformation energies required for formation of the bridging structure **A7** are significantly different for Chirik-type and Fryzuk-type complexes. For the Chirik-type complex, the formation of the H-bridged **0_Ch_A7** structure requires 62.3 kcal/mol deformation energy, whereas the formation of its Fryzuk-type analogue, **i_Fr_A7**, needs only 33.2 kcal/mol. In other words, the **0_Ch_1** complex requires approximately 2 times more deformation energy for formation of the H-bridged isomer than the **i_Fr_1** complex. Thus, the energy decomposition analysis allowed us to conclude that Chirik-type complexes have more rigid ligand environment than Fryzuk-type complexes. The more rigid ligand environment of the Chirik-type complexes makes the H-bridged complex **A7** energetically unfavorable. In the case of Fryzuk-type complexes, the ligands are more flexible and make the formation of H-bridging structures favorable. As shown above, the H-bridged complex requires higher energy barriers for the second H₂ addition than their non-H-bridged analogues. Therefore, one may conclude that a rigid ligand environment, requiring more deformation energy, favors the dinitrogen hydrogenation reaction.

- (19) Chirik, P.; Henling, L. M.; Bercaw, J. E. *Organometallics* **2001**, *20*, 534.
 (20) Pool, J. A.; Bernskoetter, W. H.; Chirik, P. J. *J. Am. Chem. Soc.* **2004**, *126*, 14326.
 (21) Pool, J. A.; Lobkovsky, E.; Chirik, P. J. *J. Am. Chem. Soc.* **2003**, *125*, 2241.
 (22) Kitaura, K.; Sakaki, S.; Morokuma, K. *Inorg. Chem.* **1981**, *20*, 2292. Morokuma, K.; Kitaura, K. In *Chemical Applications of Atomic and Molecular Electrostatic Potentials*; Politzer, P., Truhlar, D. G., Eds.; Plenum Press: New York, 1981.

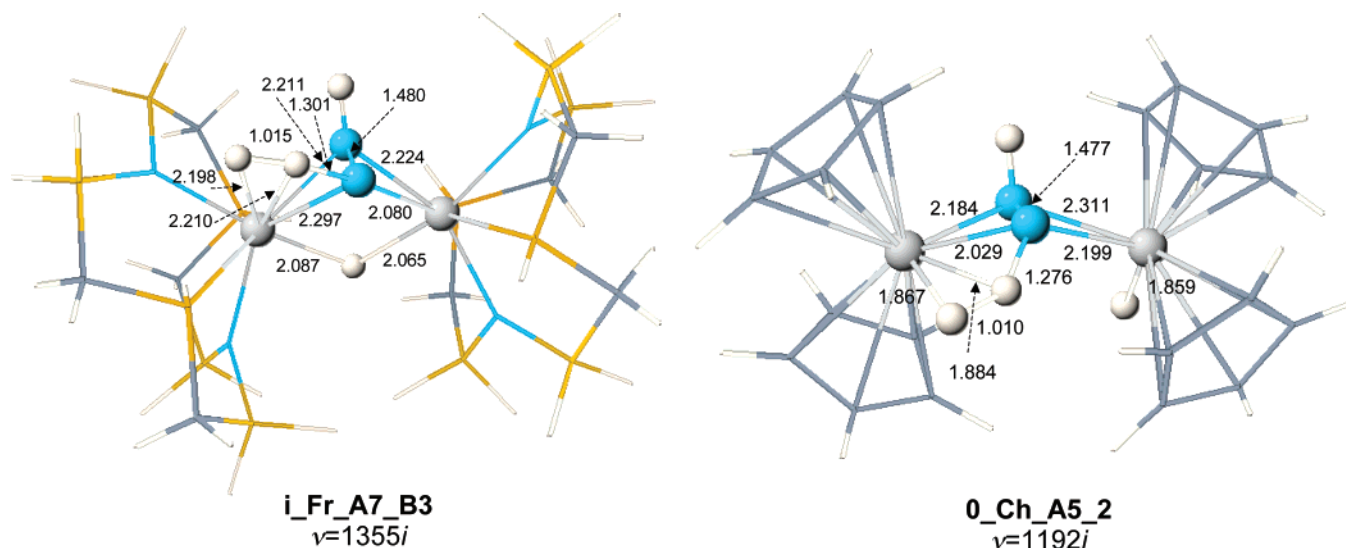


Figure 8. B3LYP/CEP-31G(d_N) optimized structures of the transition states **0_Ch_A5_2** and **i_Fr_A7_B3** of the second H₂ addition to Fryzuk- and Chirik-type complexes, respectively.

The above conclusion disagrees with the recent paper by Miyachi et al.¹⁶ Those authors calculated the mechanism of H₂ addition to the Chirik-type **0_Ch_1** complex and compared it with the mechanism of the Fryzuk-type **s_Fr_1** complex, as reported by Basch et al.⁶ On the basis of general chemical sense alone, they assumed that Chirik-type complexes have a mechanically more flexible ligand environment and drew the conclusion that ligand flexibility favors H₂ addition. However, our energy decomposition calculations lead to the opposite conclusion. Fryzuk-type complexes have a more flexible ligand environment that allows the formation of a H-bridged structure, which requires a higher energy barrier for the second H₂ addition. The Chirik-type complexes have a more rigid ligand environment, which requires higher deformation energy for formation of a H-bridged structure and favors the formation of a non-H-bridged structure, which easily adds the second H₂ molecule.

The large stability of the H-bridged complex **A7** with respect to the non-H-bridged ones, **A3/A5**, is only one of the reasons for the crucial difference in the energetic barriers of Fryzuk-type and Chirik-type reactions of the second H₂ addition. The Fryzuk-type transition state, **i_Fr_A7_B3**, is much less stable than the Chirik-type transition state, **0_Ch_A5_2**. To understand the reason behind this phenomenon, we performed a simplified energy decomposition analysis of **i_Fr_A7_B3** and **0_Ch_A5_2** and decomposed the interaction energy with the H₂ molecule into deformation energy, *DEF*, and pure interaction energy, *INT*. The required deformation of **i_Fr_A7** and **0_Ch_A5** to bind H₂ and form the respective transition states is too small to show the differences in the ligand rigidity. Both deformation energies have similar values (12.5 vs 8.7 kcal/mol). However, the pure interaction energy is very different. It is only 0.8 kcal/mol for the Fryzuk-type transition state, **i_Fr_A7_B3**, and 19.4 kcal/mol for the Chirik-type, **0_Ch_A5_2**, respectively.

The structures of the two complexes are shown in Figure 8. The difference in the pure interaction energies is caused by the fact that there is a stronger Zr–H₂ interaction in the case of **0_Ch_A5_2**. The Zr–H bonds are much shorter in **0_Ch_A5_2** than in **i_Fr_A7_B3**. This could be expected on the basis of the fact that the Zr atom in **i_Fr_A7_B3** participates in one additional interactions with the bridging H atom.

The different aptitude for formation of H-bridged structures could be also seen clearly from the products of the second H₂ addition (Figure 6). Indeed, the product of the second H₂ addition may have several isomers, which differ in the positions of two N–H and two Zr–H bonds. Calculations show that cis orientation of the N–H bonds is more favorable than their trans orientation for both series; for the Chirik-type system the isomer corresponding to trans orientation of the N–H bonds is energetically less favorable, while it is not stable at all for the Fryzuk-type system. The orientation of the Zr–H bonds is more interesting. One of the two H atoms could either bind to one Zr center, as in structure **2**, or bridge two Zr centers, as in structures **B3**, **B5**, and **B7**. The other H atom could be in a syn (**B3**), anti (**B5**), or bridging position (**B7**). As already discussed, structure **0_Ch_2**, with two terminal H ligands, is very stable. However, as could be expected from the aforementioned discussion, its analogue, **i_Fr_2**, for the Fryzuk-type systems is the least favorable among all isomers of the second H₂ addition product. For the Fryzuk-type system, the structure **i_Fr_B7**, with two H bridges, is the most stable isomer. This once again manifests that Fryzuk-type complexes tend to form H-bridges, while Chirik-type complexes prefer to form products with terminal Zr–H bonds.

3.4. What Are the Necessary Conditions for Successful Hydrogenation of the Coordinated N₂ Molecule? Numerous studies, both theoretical^{1f,6,9,24} and experimental,^{3–5,8,19,21} suggest that successful hydrogenation of the coordinated N₂ molecule is controlled by several factors. The first of them is the formation of a (μ_2, η^2, η^2 -N₂) side-on coordinated complex of N₂ with two transition metal centers. It was demonstrated^{1f} that the side-on (η^2) coordination of N₂ is electronically most suitable for its hydrogenation. The end-on (η^1) coordination of N₂ to the transition metal center(s) is not suitable for its hydrogenation and can lead to formation of ammonia (or other N-containing species) via the protonation and reduction mechanism (Chatt

(23) Chatt, J.; Pearman, A. J.; Richards, R. L. *Nature* **1975**, 253, 39. Yandulov, D. V.; Schrock, R. R. *Science* **2003**, 76, 301. Schrock, R. R. *Acc. Chem. Res.* **2005**, 38, 955.

(24) Musaev, D. G.; Basch, H.; Morokuma, K. In *Computational Modeling of Homogeneous Catalysis*; Maseras, F., Lledós, A., Eds.; Kluwer Academic Publishers: Dordrecht, 2002.

mechanism).²³ This conclusion is also supported by experiments described by Manriquez and Bercaw⁸ and Pool, Lobkovsky, and Chirik.⁴ Manriquez and Bercaw⁸ have reported that, in the complex $[(\eta^5\text{-C}_5\text{Me}_5)_2\text{Zr}]_2(\mu_2, \eta^1, \eta^1\text{-N}_2)$, with five methyl-substituted Cp ligands, the N_2 molecule is in end-on (η^1) coordination mode, and addition of H_2 molecules to this complex results in loss of N_2 . In contrast, Pool, Lobkovsky, and Chirik⁴ have reported that, in the complex $[(\eta^5\text{-C}_5\text{Me}_4\text{H})_2\text{Zr}]_2(\mu_2, \eta^2, \eta^2\text{-N}_2)$, with four methyl-substituted Cp ligands, the N_2 molecule is in side-on (η^2) coordination mode, and addition of H_2 molecules to this complex results in formation of N–H bonds. In our recent theoretical studies,⁹ we have clearly demonstrated that the reason for this remarkable difference in the reactivity of $[(\eta^5\text{-C}_5\text{Me}_5)_2\text{Zr}]_2(\mu_2, \eta^1, \eta^1\text{-N}_2)$ and $[(\eta^5\text{-C}_5\text{Me}_4\text{H})_2\text{Zr}]_2(\mu_2, \eta^2, \eta^2\text{-N}_2)$ is in the coordination mode of the N_2 molecule in these complexes, which is a result of the increased steric repulsion between the Cp'Zr fragments upon increasing the number of methyl substituents in the Cp' rings from four to five. Our theoretical studies⁹ also showed that the N_2 molecule in the dizirconium side-on coordinated complex has a substantially longer N–N bond than in the corresponding monozirconium side-on complex. Longer N–N bonds are associated with smaller HOMO–LUMO gap, higher N atomic charges, and higher population on the N_2 π^* orbitals and are a clear indication of more extensive activation of the N–N bond; mononuclear side-on coordinated complexes cannot activate the N_2 molecule enough.

The formation of the side-on (η^2) coordination complex of N_2 with two transition metal centers is not the only factor that could control the hydrogenation of N_2 . Indeed, the $[\text{rac-BpZr}]_2(\mu_2, \eta^2, \eta^2\text{-N}_2)$ complex, where the N_2 is in side-on coordination mode, does not add H_2 to N_2 under mild experimental conditions (25 °C).¹⁹ It is worth noting that the N–N bond in this complex is only 1.241 Å, suggesting the N_2 molecule is not well activated.

This indicates that some other factors, coupled with the side-on coordination of N_2 , are also important for successful hydrogenation of the coordinated N_2 molecule. As could be expected from simple molecular orbital analysis,^{1f,24} any factor (including, but not limited to, ligand effect and steric repulsion leading to conformational changes) resulting in availability of suitable HOMO ($\pi(\text{M}-\text{N}_2-\text{M})$) and LUMO ($\sigma^*(\text{M})$) orbitals of transition metal complexes of the side-on coordinated N_2 molecule would be crucial for its successful hydrogenation. As shown by Pool, Bernskoetter, and Chirik,²⁰ in Chirik-type complexes, $[(\eta^5\text{-C}_5\text{Me}_n\text{H}_{5-n})_2\text{Zr}]_2(\mu_2, \eta^2, \eta^2\text{-N}_2)$ for $n = 0$ and 4, this can be achieved by twisting of the zirconocene edges. This is true also for the complex $[(\eta^5\text{-C}_5\text{H}_5\text{-1,3-(SiMe}_3)_2)_2\text{Zr}]_2(\mu_2, \eta^2, \eta^2\text{-N}_2)$, where the zirconocene edges are not twisted (twisting angle, $\theta = 0^\circ$). This complex does not add H_2 under the conditions of the experiment.²¹

However, experimental studies indicate that the side-on coordination of N_2 and the availability of suitable HOMO and LUMO orbitals (caused, in particular, by zirconocene edges twisting in several Cp-containing dizirconium complexes, including Chirik-type complexes) are not the only factors that affect the successful hydrogenation of the coordinated N_2 molecule. For example, in $[\text{rac-BpZr}]_2(\mu_2, \eta^2, \eta^2\text{-N}_2)$, (a) the N_2 molecule is in its side-on coordination mode and (b) the zirconocene edges are twisted at 46° (this value is close to the

49° reported for **0_Ch_1**⁹), which makes the HOMO and LUMO suitable for hydrogenation (see Figure 3S of the Supporting Information). However, although this complex satisfies the above two conditions, it does not hydrogenate the N_2 molecule under the experimental conditions.¹⁹

The above examples clearly indicate that there are other factors which need to be taken into account upon study of hydrogenation of the coordinated N_2 . The present study indicates that one of them is the rigidity of the ligand environment and the aptitude for formation of H-bridged structures. If the ligand environment of the Zr centers is flexible, then the first H_2 addition could lead to a H-bridged structure (instead of the structure with a terminal H), which usually requires a large barrier for the second H_2 addition. In contrast, if the ligand environment of the Zr centers is rigid, then the required large deformation energy prevents the formation of the H-bridged complex and results in the formation of a non-H-bridged complex, which usually requires a smaller barrier for the second H_2 addition.

The future candidate complexes for more effective N_2 hydrogenation should be tested not only for N_2 coordination mode (side-on vs end-on) and availability of the frontier molecular orbitals, but also for the rigidity of their ligand environment and the relative stability of the H-bridged and non-H-bridged isomers of the first H_2 addition product.

It should be noted that additional conditions for successful N_2 hydrogenation possibly exist. Such possibilities are currently under investigation in our laboratory.

4. Conclusions

Detailed computational study of the mechanism of dinitrogen hydrogenation in the Chirik-type complex $[(\eta^5\text{-C}_5\text{Me}_4\text{H})_2\text{Zr}]_2(\mu_2, \eta^2, \eta^2\text{-N}_2)$, **4_Ch_1**, and the Fryzuk-type complex $\{[\text{PhP}(\text{CH}_2\text{SiMe}_2\text{NSiMe}_2\text{CH}_2)_2\text{PPh}]_2\text{Zr}\}_2(\mu_2, \eta^2, \eta^2\text{-N}_2)$, **Fr_1**, shows that the experimentally observed difference in their reactivity^{3,4} is due to the different rigidity of their ligand environments, which causes different relative stability of H-bridged (**A7**) and non-H-bridged (**A3/A5**) intermediates. In the case of the **4_Ch_1** complex, the second H_2 addition starts from the less stable **A3/A5** complexes and proceeds with a smaller energy barrier than the first H_2 addition. In contrast, in the case of the **Fr_1** complex, the second H_2 addition starts from the more stable H-bridged **A7** complex and requires a much larger energy barrier than the first H_2 addition. In addition, the existence of a hydrogen bridge results in much higher energy of the Fryzuk-type transition state of the second H_2 addition than the respective Chirik-type transition state due to decreased availability of the Zr center to interact with the incoming H_2 molecule.

Our calculations indicate that H_2 addition to $[(\eta^5\text{-C}_5\text{Me}_n\text{H}_{5-n})_2\text{Zr}]_2(\mu_2, \eta^2, \eta^2\text{-N}_2)$ ($n = 0, 4, 5$; $n = 5$ is hypothetical) and $[(\eta^5\text{-C}_5\text{H}_5\text{-1,2,4-Me}_3)(\eta^5\text{-C}_5\text{Me}_5)_2\text{Zr}]_2(\mu_2, \eta^2, \eta^2\text{-N}_2)$ follows similar mechanisms. In agreement with the experiment,⁵ the number of methyl groups does not significantly affect the barrier of the first H_2 addition. However, increasing number of methyl substituents increases steric repulsion and makes the side-on dinuclear coordination (favorable for N_2 hydrogenation) less preferable in the complex with $n = 5$. This explains why, experimentally, this complex loses N_2 upon H_2 addition.⁸

Comparison of our results with those from previous experimental^{3–5,8,19,21} and theoretical^{1f,6,9,24} studies clearly indicates the existence of several factors that are necessary for the successful hydrogenation of the coordinated N₂ molecule: (1) the side-on coordination of N₂ to two transition metal centers, (2) the availability of the HOMO and LUMO with appropriate symmetry, and (3) the rigidity of the ligand environment. The results of the present paper imply that future candidate complexes for more effective dinitrogen hydrogenation should be tested not only for N₂ coordination mode (side-on vs end-on) and availability of appropriate HOMOs and LUMOs, but also for the rigidity of their ligand environment and relative stability of the H-bridged and non-H-bridged isomers of the first H₂ addition product.

Acknowledgment. This work was supported in part by a grant (CHE-0209660) from the U.S. National Science Foundation. Computer resources were provided in part by an Air Force Office of Scientific Research DURIP grant (FA9550-04-1-0321)

as well as by the Cherry Emerson Center for Scientific Computation. D.Q.-S. thanks the Ministerio de Educación y Ciencia of Spain for postdoctoral support.

Supporting Information Available: Figures 1S and 2S, representing the equilibrium and transition-state structures for the reaction of the first, second, and third H₂ additions to [(η⁵-C₅H₅)₂Zr]₂(μ₂,η²,η²-N₂) (**0_Ch_1**) and {[HP(CH₂SiH₂NSiH₂-CH₂)₂PH]Zr}₂(μ₂,η²,η²-N₂) (**i_Fr_1**), respectively; Figure 3S, showing the calculated frontier orbitals of (a) **0_Ch_1**, (b) **4_Ch_1**, (c) [(η⁵-C₅H₅-1,3-(SiMe₃)₂)₂Zr]₂(μ₂,η²,η²-N₂), and (d) [*rac*-BpZr]₂(μ₂,η²,η²-N₂); Table 1S, addressing the reliability of the B3LYP/CEP-31G(d_N) computational approach compared to B3LYP/SDD//6-31G(d); Tables 2S, 3S, and 4S, giving the Cartesian coordinates of all calculated structures; complete ref 14. This material is available free of charge via the Internet at <http://pubs.acs.org>.

JA057937Q